Observation of x-ray magnetic circular dichroism at the Ru *K* edge in Co-Ru alloys

H. Hashizume* and K. Ishiji
Photon Factory, KEK, Tsukuba 305-0801, Japan

J. C. Lang, D. Haskel, and G. Srajer
Advanced Photon Source, Argonne National Laboratory, Argonne, Illinois 60439, USA

J. Minár and H. Ebert
Department Chemie und Biochemie, Physikalische Chemie, Universität München, München D-81377, Germany
(Received 16 January 2006; revised manuscript received 19 April 2006; published 13 June 2006)

X-ray magnetic circular dichroism spectra have been measured from dilute Ru alloys of Co at the Ru *K* edge, evidencing the induced magnetization on Ru in contact with ferromagnetic Co. This was made possible using circularly polarized probing beams of approximately 22 keV in energy obtained from a germanium Laue-reflection phase retarder at a synchrotron source. The Ru dichroism is quite small with a main peak of -3×10^{-4} in flipping ratio at about 6 eV above the *K* absorption edge. The spectrum has a very similar profile to the one of the Co *K*-edge dichroism. *Ab initio* calculations indicate that the Ru dichroism is generated by the *p*-orbital magnetic moment on the core-hole site, which is induced through the *p-d* hybridization between Co and Ru.

DOI: 10.1103/PhysRevB.73.224416 PACS number(s): 75.30.Et, 07.85.Qe, 75.47.Np, 75.70.−i

I. INTRODUCTION

Among various magnetic/nonmagnetic-layered structures of metals, Co/Ru is one of the strongest in the interlayer exchange coupling.[1] This system is of fundamental interest and finds practical applications in synthetic antiferromagnetic layers[2] for spin valves. Ferromagnetic Co moments in Co/Ru multilayers couple with each other either parallel or antiparallel depending on the spacer Ru thickness (t_{Ru}). This has been evidenced using various approaches including magnetometry,[1,3–7] magnetoresistance,[6,7] magneto-optical Kerr effect,[8] x-ray magnetic circular dichroism (XMCD),[9] and spin-resolved photoemission measurements.[10] Most of the investigations find consistently approximately 1.0 nm in t_{Ru} for the period of the oscillatory coupling. In the Ruderman-Kittel-Kasuya-Yosida-like theories including the quantum-interference model,[11,12] the interlayer coupling of the ferromagnetic Co moments is mediated by conduction electrons in the nonmagnetic spacer Ru layers, which become spin polarized by magnetic interactions with Co at the interface. The polarization propagates across the Ru layer and interacts with another Co layer, thereby giving rise to a coupling between the Co moments.

With this in mind, Rampe *et al.*[10] observed spin asymmetries of valence electrons near the Fermi level in 1 atomic-layer Ru grown on Co(0001) surface by photoemission spectroscopy. Harp *et al.*[13] failed, however, to verify the magnetic polarization of Ru in Co-Ru alloys by x-ray magnetic circular dichroism measurements at the *M* edge and concluded that the peak flipping ratio χ_p of the XMCD signal is no greater than 0.005, corresponding to a magnetic moment of 0.03 μ_B per Ru atom. This is in contrast with the large magnetic moment of 0.7 μ_B reported for adlayers of Ru on Fe(100) surface.[14] The latter was derived from spin-polarized Auger electron spectroscopy measurements, which show as well that the polarization is concentrated in an interface region of 1 atomic-layer thickness. The XMCD observed from Ru/Fe(001) multilayers at the Ru *M* and *L* edges[8,15] proves the magnetic polarization of the Ru 4*d* states. However, the *K*-edge dichroism has never been observed, from either alloys or thin films, which probes the Ru 5*p* states via dipole $1s\rightarrow5p$ transition. These states are delocalized and hence more pertinent to the exchange coupling in layered Co/Ru and Fe/Ru structures. The lack of reports appears to be due to the technical difficulty in producing circularly polarized x-rays of energy as high as 22.1 keV (Ru *K* edge).

II. LAUE-TYPE X-RAY PHASE RETARDER

In the present study we designed a Laue-type x-ray phase retarder using the symmetrically equivalent (220) and $(2\bar{2}0)$ reflections of a Ge crystal,[16] which allowed us to observe magnetic dichroism signals from Co-Ru alloys at the Ru *K* edge. The phase retarder is a 600-μm-thick germanium plate, slightly thinner than the optimum thickness for a three-quarter-wavelength phase plate at 22 keV. This retarder was used to convert the linearly polarized light (third harmonic) from the 4-ID-D undulator of the Advanced Photon Source (APS), Argonne National Laboratory, to circularly polarized x-rays. In our setup, the (220) reflection scattered x-rays upwards and inboard (in the direction of the APS storage ring), whereas the $(2\bar{2}0)$ reflection scattered upwards and outboard (away from the storage ring) (Fig. 1). The (220) and $(2\bar{2}0)$ reflections thus produce a circularly polarized beam of − and + helicities, respectively.[16] The forward diffracted O beam was used in the experiment, whose degree of circular polarization was experimentally determined to be approximately 75%. The phase retarder provides a circular polarization of a maximal degree at only one specific energy. Over the energy range of the XMCD scan, however, the polarization rate only varies by less than a few percents. We focused the x-ray

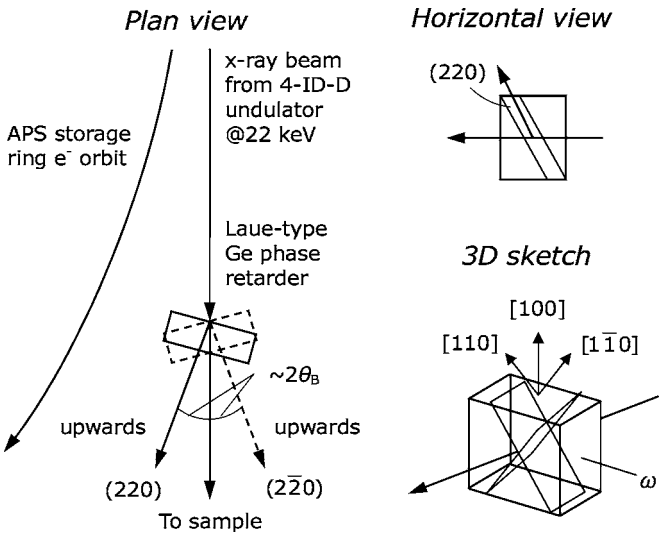

FIG. 1. Experimental setup on the APS 4-ID-D beam line. The 4-ID-D monochromator and the focusing optics are not shown. The active (220) and (2$\bar{2}$0) planes in the germanium phase retarder are inclined by 45° to the horizontal synchrotron plane. In this setup, circularly polarized x-ray beams of + and − helicities are produced by the (2$\bar{2}$0) and (220) reflections, respectively. Rotating the retarder around the horizontal ω axis scans the x-ray energy. The APS storage ring was filled with 324 electron bunches on the orbit at the time of experiment.

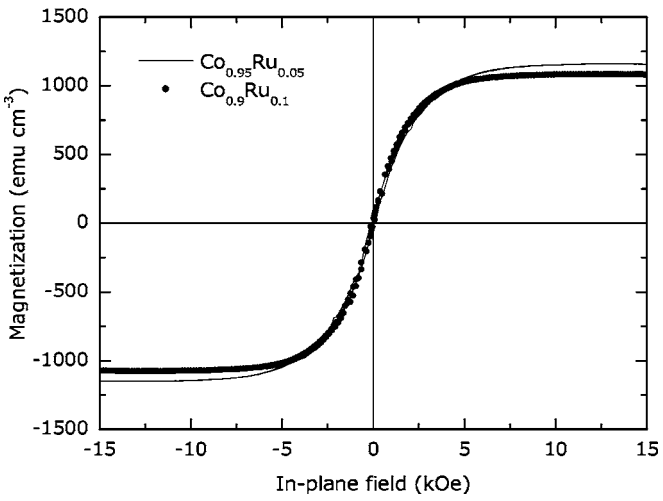

FIG. 2. Magnetization curves for the $Co_{0.95}Ru_{0.05}$ and $Co_{0.9}Ru_{0.1}$ samples. Measured with a vibrating-sample magnetometer applying an in-plane field. Openings of the hysteresis loops near zero fields are not visible on the scale of the diagram.

beam after the phase retarder to 0.2 mm vertical and 0.3 mm horizontal at the sample. This beam illuminated a Co-Ru sample at a 45° glancing angle in the transmission geometry, placed in the air gap of an electromagnet. The energy resolution of our XMCD measurement is better than 3 eV.

III. SAMPLES AND XMCD MEASUREMENT

Our samples are random Co-Ru alloys of nominal composition $Co_{0.95}Ru_{0.05}$ and $Co_{0.9}Ru_{0.1}$, synthesized by arc melting Co and Ru metals, and hot pressed in the form of foil (0.15 mm in thickness). X-ray fluorescence analyses show 5.37 and 10.11 at. % for the actual Ru compositions. The samples are predominately in the hcp phase, with the fcc content below 5% by volume. Wide-angle x-ray powder scans show no sign of the presence of intermetallic compounds. Both hcp and fcc lines are shifted towards low 2θ angles as compared with the pure Co lines, indicating lattice expansions due to the Ru alloying. The powder patterns display a (10$\bar{1}$1) texture along the sample plane. Transmission-electron-microscopy observations reveal large grains of ~10 μm size in the two samples. When magnetized in plane, the samples saturate at ~5 kOe. The saturation magnetizations are 1124 and 1066 emu cm^{-3} for the 5% Ru and 10% Ru samples, respectively, at room temperature (Fig. 2). While these are somewhat lower than the bulk Co magnetization, the saturation magnetizations of the two samples scale nicely to the Co compositions. The coercive field is as low as 50 Oe in the two samples.

Figure 3 shows the nonmagnetic and magnetic absorption spectra observed from our samples. We measured the dichroism signals by flipping a magnetic field (7.2 kOe) pro and contra along the x-ray **k** vector for a fixed photon helicity. We define XMCD by $\Delta\mu t/\mu t_{\text{jump}}$, where $\Delta\mu=\mu(-,+)-\mu(+,+)$. Here μ is the linear absorption coefficient and the signs in the first and second places in the parentheses represent the field direction and the photon helicity, respectively. We define the + field parallel to the x-ray **k** vector. μt_{jump} is the measured jump height in μt at the K edge. We note in Fig. 3 that the observed μt_{jump} values, 0.89 and 1.67, scale exactly to the alloying compositions of Ru in the samples. The raw dichroism data are affected by energy-dependent backgrounds, which we remove by calculating the difference of the two spectra, measured using opposite photon helicities (Fig. 3). In principle, flipping the photon helicity for a fixed direction of applied field allows the same data to be obtained. We optioned the field flip for a practical reason to avoid energy shifts produced when the phase retarder is misaligned from the exact diffraction position.[16] The retarder is in an energy dispersive geometry (scattering planes at 45°) with respect to the 4-ID-D double-crystal Si(111) monochromator. If each of the (220) and (2$\bar{2}$0) reflections is not exactly aligned, there is a small energy shift in the transmitted O beams when switching between the (220) and (2$\bar{2}$0) reflections. This energy shift is small but even a very small shift (50 meV) can cause a large artifact in the dichroism data. Note that this is not a problem with a diamond Bragg-reflection phase retarder in wide use because it is operated on the tails of a reflection and therefore not enough of the beam is scattered to change the average energy of the transmitted beam. We scanned the magnetic field to trace a loop of $0\rightarrow+7.2\rightarrow0\rightarrow-7.2\rightarrow0$ kOe every 8 s while an ion chamber was measuring the transmitted x-rays after a sample. At this scan rate, the use of the lock-in technique[17] would improve trivially the signal-to-noise ratio of the dichroism signal.

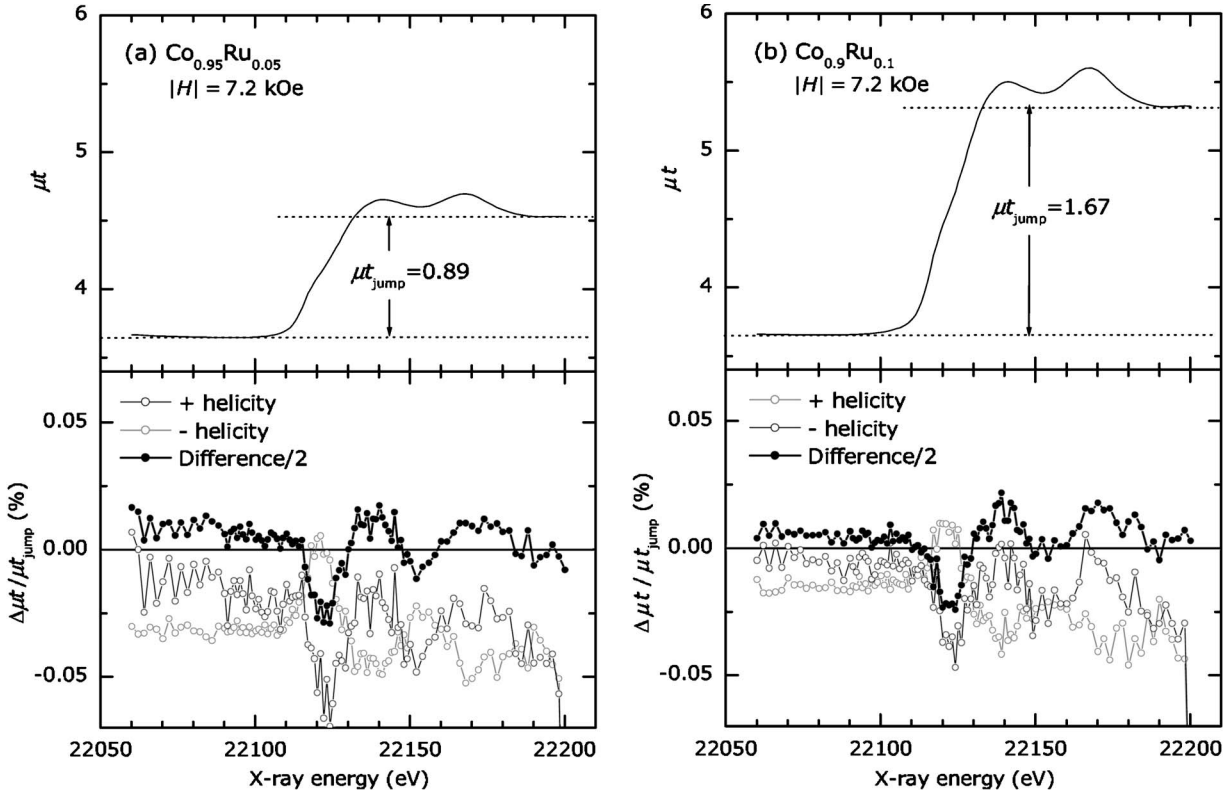

FIG. 3. Nonmagnetic (top panel) and magnetic (bottom panel) x-ray absorption spectra measured from the $Co_{0.95}Ru_{0.05}$ (a) and $Co_{0.9}Ru_{0.1}$ (b) samples near the Ru K edge. In the bottom panel, open circles show raw data obtained using the circularly polarized beams of + and − helicities, whereas filled circles show the differences divided by 2, giving the background-free dichroic spectra. X-ray count time per energy point is 320 s (a) and 128 s (b). Data collection time: 20 h (a) and 12 h (b).

IV. RESULTS

The XMCD spectra observed at the Ru K edge are quite weak, approximately -3×10^{-4} in peak flipping ratio (χ_p), and featured by the pronounced oscillatory structure in the 10–100 eV range off edge (Fig. 4). The 5% Ru and 10% Ru samples exhibit indistinguishable spectra. The nearly equal χ_p values on one hand and the μt_{jump} ratio in agreement with the Ru concentration ratio on the other hand indicate that all Ru atoms in the samples are magnetic and contribute to the dichroism. In addition, the magnetic moment per Ru atom does not depend on the chemical composition in the range investigated. This suggests that Ru atoms are dispersed in the Co matrix without forming clusters and in contact with ferromagnetic Co. This is in line with the miscibility of Co and Ru over the whole concentration range.[18]

In Fig. 4 we overlay a scaled version of an XMCD spectrum observed from a Co/Cu multilayer at the Co K edge.[19] The thickness of our Co-Ru alloy samples was not suitable for measurements at the Co K edge. When displayed on the $E-E_0$ scale, where E_0 is the edge energy (22 117 eV for Ru and 7709 eV for Co), the Ru and Co spectra fit each other surprisingly well. The similar Co and Ru spectra are in contrast with the distinct Co and Cu spectra measured from Co/Cu multilayers at the K edges; there, the Cu dichroism shows a main peak and oscillation features significantly narrower than the Co spectrum. This was ascribed to the incomplete screening of the core holes by $s+p$ electrons in Cu where the d electrons are quenched.[19] The magnitude of the Ru K-edge dichroism (χ_p) observed in the present samples (-3×10^{-4}) almost equals that of the Cu K-edge dichroism from a Co/Cu multilayer at the second antiferromagnetic peak of the coupling oscillation.[19] This is rather intriguing since the interlayer coupling energies of Co/Cu and Co/Ru

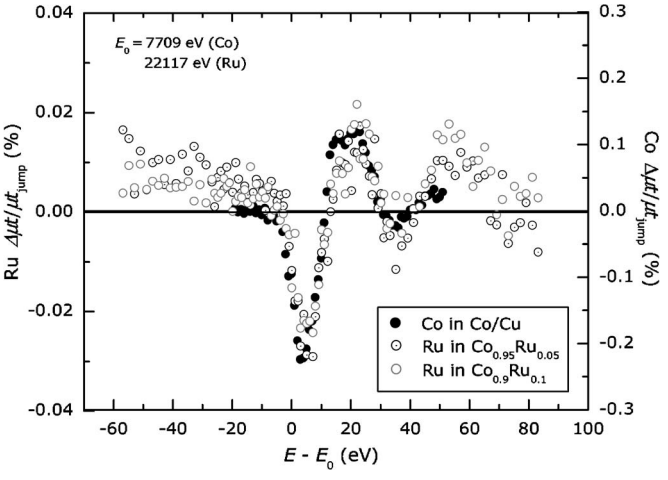

FIG. 4. Comparing the dichroic spectra from the $Co_{0.95}Ru_{0.05}$ and $Co_{0.9}Ru_{0.1}$ samples at the Ru K edge with the one from a Co/Cu multilayers at the Co K edge. E_0: absorption-edge energy. Note that the dichroism from induced magnetizations on Ru is one order of magnitude smaller than the one from ferromagnetic Co.

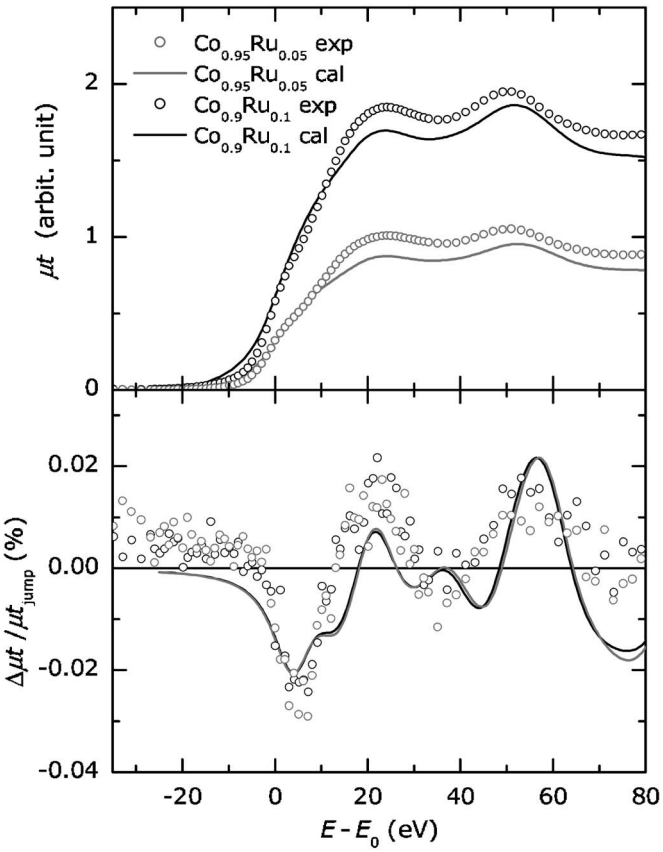

FIG. 5. Experimental (circles) and calculated (lines) XAS (top panel) and XMCD (bottom panel) spectra near the Ru K edge (E_0=22.117 keV).

multilayers are very different, 0.3 erg cm^{-2} versus 5 erg cm^{-2} at the first antiferromagnetic peak.[1] It is to be seen whether Ru thin films sandwiched between Co layers show similar spectra to those given in Fig. 4.

V. THEORETICAL CALCULATIONS

To support our experimental results, we performed first-principle calculations of nonmagnetic (XAS) and magnetic absorption spectra using the local-density approximation of the density functional theory. We employed the spin-polarized relativistic Korringa-Kohn-Rostoker formalism with the coherent potential approximation[20,21] for the hcp phase of the disordered $Co_{1-x}Ru_x$ alloys (x=0.0537 and 0.1011). Self-consistent potentials were calculated by assuming the experimental lattice constants (a=0.2520 nm, c=0.4078 nm for the 5% Ru sample), but a marginal effect of the lattice expansion was found on the XMCD spectra. To make a direct comparison feasible, we present in Fig. 5 the theoretical spectra for Ru convoluted with a Lorentzian of 5.3 eV in full width at half maximum (FWHM) (Ref. 22) and a Gaussian of 1 eV in FWHM, accounting for the finite core-hole lifetime and the experimental resolution, respectively. The features of the experimental XAS and XMCD spectra are reproduced well by the theoretical calculation, although the latter shows more structures. We calculated the spectra within the dipole approximation, as we do not see any quadrupole feature in the pre-edge nor near-edge regions of the observed spectra. These features appear to have been be smeared out by the short core-hole lifetime of Ru.

TABLE I. Orbital-resolved spin (μ_s) and orbital (μ_o) magnetic moments (in μ_B/atom) for Co and Ru in $Co_{1-x}Ru_x$ alloys.

		Co		Ru	
x		μ_s	μ_o	μ_s	μ_o
0.0537	s	−0.012	0	−0.017	0
	p	−0.054	0.001	−0.047	0.001
	d	1.614	0.072	0.263	−0.018
	Sum	1.548	0.073	0.199	−0.017
0.1011	s	−0.011	0	−0.016	0
	p	−0.048	0.001	−0.044	0.001
	d	1.566	0.071	0.175	−0.017
	Sum	1.507	0.071	0.115	−0.016

The corresponding spin and orbital moments are given in Table I for $Co_{1-x}Ru_x$. The magnetic moment of Co is slightly reduced from the pure Co value, whereas Ru acquires a total spin magnetic moment of 0.1–0.2 μ_B and a total orbital magnetic moment of approximately −0.02 μ_B. We note in Table I that the p-orbital magnetic moments are similar for Ru and Co. One may inquire whether this is consistent with the much weaker Ru dichroism than the Co dichroism observed in Fig. 4, since the K-edge dichroism is predominantly due to the p-orbital magnetic moment on the core-hole site.[23] In fact, the nonbroadened theoretical Ru spectra have comparable amplitudes with the nonbroadened Co spectra. In Fig. 5 the Ru spectra is reduced considerably because of the large width of the broadening function due to the short core-hole lifetime (5.3 eV).

The local densities of states are shown in Fig. 6 for Ru. In the calculation we found strong hybridizations between the unoccupied p states of Co and Ru. Furthermore, the orbital

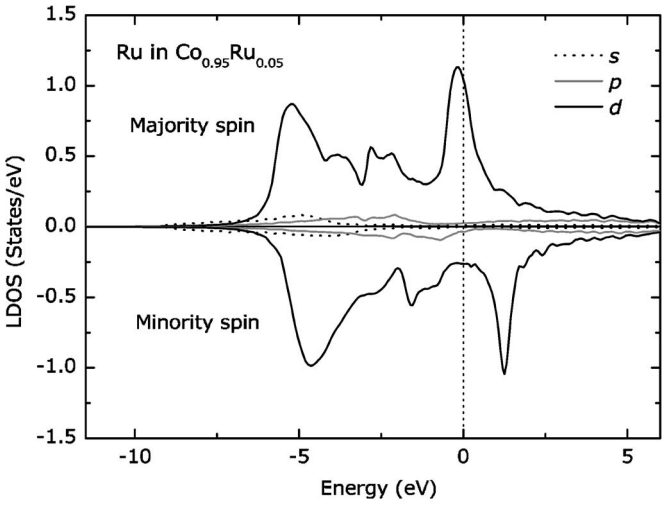

FIG. 6. Local density of states (LDOS) including small s and p contributions for $Co_{0.95}Ru_{0.05}$ alloy.

polarizations of Co and Ru showed analogous oscillations. This explains the similar XMCD profiles for Co and Ru observed in Fig. 4. The Ru dichroism is generated through the spin-orbit interaction (SOI) on the absorbing atoms. Switching off the SOI on the Ru site reduces the XMCD signal by a factor of 100. This evidences that the origin of the Ru dichroism is the Ru orbital magnetic moment. On the other hand, switching off the SOI on neighboring Co sites has marginal effects on the Ru dichroism, indicating that the mechanism claimed by Igarashi and Hirai[24] for the *K*-edge dichroism of Fe and Ni is unimportant in the Co-Ru alloy. It is true that Ru is polarized magnetically by the *p*-*d* hybridization between Co and Ru. However, the Ru 5*p*-orbital moment is not induced directly by the 3*d*-orbital moment on the neighboring Co sites, but probably by the Ru 5*p*-spin moment that is generated by the Co 3*d*-spin moment through the *p*-*d* hybridization.

VI. CONCLUDING REMARKS

The successful operation of the high-energy Laue-reflection phase retarder in the present study paves a way to exploring the role of the induced Ru magnetization in strongly coupled Co/Ru multilayers as compared with that of the Cu magnetization in weakly coupled Co/Cu. Ru is reported to retain much larger magnetic moments when placed in Fe alloys or layered with Fe thin films than in Co alloys and Co/Ru multilayers.[8,14,25] This behavior, once discussed in terms of "*d*-band occupation number,"[13] can be investigated using the x-ray technique developed in this study. The technique offers an advantage of element specificity, which allows induced magnetizations on Ru to be probed selectively in the presence of ferromagnetic backgrounds from other elements. This is not feasible with neutron scattering. The present study opens a door to x-ray studies of the magnetism of 4*d* metals Tc, Ru, Rh, and Pd (Refs. 26–30) by resonant absorption and scattering[31] at the *K* edge.

ACKNOWLEDGMENTS

The authors thank Y. Obi, S. Hanada, and K. Takanashi for assistances in sample preparation, the Rigaku Corporation for the fluorescence analysis, K. Mibu for the measurement of the magnetization curves, T. Ida for the collection of x-ray diffraction data, and H. Yasuda for the electron microscopy observation. The work at the Advanced Photon Source is supported by the U.S. DOE, Office of Science, Contract No. W-31-109-ENG-38. The theoretical part is supported by the German BMBF, Contract No. FKZ 05 KS1WMB/1.

*Author to whom correspondence should be addressed.
Electronic address: hhashizu@mbg.ocn.ne.jp

[1] S. S. P. Parkin, Phys. Rev. Lett. **67**, 3598 (1991).
[2] J. L. Leal and M. H. Kryder, J. Appl. Phys. **83**, 3720 (1998).
[3] S. S. P. Parkin, N. More, and K. P. Roche, Phys. Rev. Lett. **64**, 2306 (1990).
[4] K. Ounadjela, A. Arbaoui, A. Herr, R. Poinsot, A. Dinia, D. Muller, and P. Panissod, J. Magn. Magn. Mater. **106**, 1896 (1992).
[5] P. J. H. Bloemen, H. W. van Kesteren, H. J. M. Swagten, and W. J. M. de Jonge, Phys. Rev. B **50**, 13505 (1994).
[6] S. Colis, A. Dinia, D. Deck, G. Schmerber, and V. Da Costa, J. Appl. Phys. **88**, 1552 (2000).
[7] S. Zoll, A. Dinia, J. P. Jay, C. Mény, G. Z. Pan, A. Michel, L. El Chahal, V. Pierron-Bohnes, P. Panissod, and H. A. M. Van den Berg, Phys. Rev. B **57**, 4842 (1998).
[8] T. Lin, M. A. Tomaz, M. M. Schwickert, and G. R. Harp, Phys. Rev. B **58**, 862 (1998).
[9] Y. Wu, S. S. P. Parkin, J. Stöhr, M. G. Samant, B. D. Hermsmeier, S. Koranda, D. Dunham, and B. P. Tonner, Appl. Phys. Lett. **63**, 263 (1993).
[10] A. Rampe, D. Hartmann, W. Weber, S. Popovic, M. Reese, and G. Güntherodt, Phys. Rev. B **51**, 3230 (1995).
[11] P. Bruno and C. Chappert, Phys. Rev. Lett. **67**, 1602 (1991).
[12] P. Bruno, Phys. Rev. B **52**, 411 (1995).
[13] G. R. Harp, S. S. P. Parkin, W. L. O'Brien, and B. P. Tonner, J. Appl. Phys. **76**, 6471 (1994); Phys. Rev. B **51**, 12037 (1995).
[14] K. Totland, P. Fuchs, J. C. Gröbli, and M. Landolt, Phys. Rev. Lett. **70**, 2487 (1993).
[15] M. A. Tomaz, T. Lin, G. R. Harp, and E. Hallin, J. Vac. Sci. Technol. A **16**, 1359 (1998).
[16] J. C. Lang, D. Haskel, G. Srajer, H. Hashizume, and K. Ishiji (unpublished).
[17] M. Suzuki, N. Kawamura, and T. Ishikawa, Proc. SPIE **4145**, 140 (2001).
[18] T. B. Massalski, in *Binary Alloy Phase Diagram*, 2nd ed., edited by T. B. Massalski, H. Okamoto, P. R. Subramanian, and L. Kacprza (American Society of Metals, Metals Park, OH, 1990).
[19] S. Nagamatsu, H. Matsumoto, T. Fujikawa, K. Ishiji, and H. Hashizume, Phys. Rev. B **70**, 174442 (2004).
[20] H. Ebert, in *Electronic Structure and Physical Properties of Solids, Lecture Notes Phys.*, Vol. 535, edited by H. Dreysse (Springer, Berlin, 2000), p. 191.
[21] H. Ebert, Rep. Prog. Phys. **59**, 1665 (1996).
[22] M. O. Krause and J. H. Oliver, J. Phys. Chem. Ref. Data **8**, 329 (1979).
[23] H. Ebert, J. Minár, and V. Popescu, in *Magnetic Dichroism in Electron Spectroscopy, Lecture Notes Phys.*, Vol. 580, edited by K. Barberschke, M. Donath, and W. Nolting (Springer, Berlin, 2001), p. 371.
[24] J. Igarashi and K. Hirai, Phys. Rev. B **50**, 17820 (1994).
[25] L. Zhong and A. Freeman, J. Appl. Phys. **81**, 3890 (1997).
[26] Z. Celinski, B. Heinrich, J. F. Cochran, W. B. Muir, A. S. Arrott, and J. Kirschner, Phys. Rev. Lett. **65**, 1156 (1990).
[27] O. Eriksson, R. C. Albers, and A. M. Boring, Phys. Rev. Lett. **66**, 1350 (1991).
[28] S. Blügel, Phys. Rev. Lett. **68**, 851 (1992).
[29] R. Wu and A. J. Freeman, Phys. Rev. B **45**, 7222 (1992).
[30] T. Kachel, W. Gudat, C. Carbone, E. Vescovo, S. Blügel, U. Alkemper, and W. Eberhardt, Phys. Rev. B **46**, 12888 (1992).
[31] Y. Hayasaki, K. Ishiji, H. Hashizume, N. Hosoito, K. Omote, K. Kuribayashi, G. Srajer, J. C. Lang, and D. Haskel, J. Phys.: Condens. Matter **16**, 1915 (2004).